



UNIVERSITI  
TEKNOLOGI  
PETRONAS

**Impact of Coal Compressibility On Coalbed Methane Production: A  
Comparison Study of Malaysian Coal to Other CBM Fields**

By

Kong Fook Ann

Softbound Report submitted in partial  
fulfilment of the requirements for the Bachelor  
of Engineering (Hons) (Petroleum  
Engineering)

May 2013

Universiti Teknologi PETRONAS

Bandar Seri Iskandar

31750 Tronoh

Perak Darul Ridzuan

## **CERTIFICATION OF APPROVAL**

### **Impact of Coal Compressibility On Coalbed Methane Production: A Comparison Study of Malaysian Coal to Other CBM Fields**

By

Kong Fook Ann

A project dissertation submitted to the Petroleum  
Engineering Department of Universiti Teknologi  
PETRONAS in partial fulfilment of the requirement  
for the BACHELOR OF ENGINEERING (Hons)  
(PETROLEUM ENGINEERING)

Approved by,

---

(MR. SALEEM QADIR TUNIO)

UNIVERSITI TEKNOLOGI PETRONAS

TRONOH, PERAK

May 2013

## **CERTIFICATION OF ORIGINALITY**

This is to certify that I am responsible for the work submitted in this project, that the original work is my own except as specified in the references and acknowledgements, and that the original work contained herein have not been undertaken or done by unspecified sources or persons.

---

(KONG FOOK ANN)

## ABSTRACT

The purpose of this research is to explain the relationship between the coal compressibility and the subsequent impact on the gas production in a coalbed methane reservoir. Coalbed methane is a type of unconventional source of petroleum, in which the methane gas is stored in the coalbed reservoirs, which act as both source rock and reservoir rock. Unlike conventional reservoir rock properties, coal has dual-porosity characteristics. 95% of the gases are stored in micropore via adsorption in the matrix of the coal, best describes with Langmuir Adsorption Isotherm. The remaining gases are stored as free gas in the macropore, also known as the cleat system of the coal, made up of butt cleats and face cleats.

After ‘dewatering’ during the production stage of coalbed methane, gases in the micropore of coal will be desorbed and flow into the cleats. At this stage, the coal undergoes several compressibility changes due to the change in effective stress and the matrix shrinkage as gases desorbed from coal matrix. The changes in the bulk compressibility, pore compressibility, matrix compressibility and matrix shrinkage compressibility will have impacts on the permeability of the coal, which ultimately have an impact on CBM production. Hence, laboratory experiments will be conducted to investigate the relationship between these compressibilities and the permeability of the coal samples. Subsequently, the production potential of the Malaysian coal samples can be determined via simulation studies and compared to other actual producing coalbed methane fields.

**Keywords:** coalbed methane, compressibility, permeability, production

## Table of Contents

CERTIFICATION OF APPROVAL .....	ii
CERTIFICATION OF ORIGINALITY .....	ii
ABSTRACT .....	iii
Table of Figures .....	vi
CHAPTER 1 - INTRODUCTION .....	1
1.1 Background of Study .....	1
1.2 Problem Statement .....	2
1.2.1 Problem Identification.....	2
1.2.2 Significance of the Project .....	2
1.3 Objectives .....	2
1.4 Scope of Study .....	3
1.5 Relevancy of the Project .....	3
1.6 Feasibility of the Project within the Scope and Time Frame.....	3
CHAPTER 2 – LITERATURE REVIEW .....	5
2.1 Formation of Coal .....	5
2.2 Coal Rank.....	6
2.3 Dual Porosity Characteristic of Coal Structure.....	7
2.4 Gas Storage and Transportation in Coal .....	9
2.5 Bulk Compressibility, Pore Volume Compressibility, Matrix Compressibility, Matrix Shrinkage Compressibility and Permeability Model of Coal .....	12
2.5.1 Bulk Compressibility .....	12
2.5.2 Pore Compressibility .....	13
2.5.3 Matrix Compressibility .....	13
2.5.4 Matrix Shrinkage Compressibility .....	13
2.5.6 Matchstick Permeability Model for Coal.....	13
2.5.7 Numerical Simulation of CBM with Eclipse .....	15
2.6 Previous Laboratory Studies on Compressibility .....	18
2.6.1 Bulk and Pore Compressibility .....	18
2.6.2 Matrix and Matrix Shrinkage Compressibility .....	19
2.6.3 Laboratory Study of Sorption Capacity of Various Gases.....	20
CHAPTER 3 - METHODOLOGY .....	22

3.1	Laboratory Study of Permeability Using PoroPerm .....	22
3.1.1	Objective of Permeability Study Using PoroPerm.....	22
3.1.2	Sample Description and Preparation .....	22
3.1.3	Experimental Procedures .....	23
3.2	Laboratory Study of Compressibility Using Point Load Test .....	24
3.2.1	Objective of Compressibility Study Using Triaxial Cell.....	24
3.2.2	Sample Description and Preparation .....	24
3.2.3	Experimental Procedures .....	24
3.3	Software Simulation Study .....	25
3.4	Flow Chart .....	26
3.5	Project Timeline/ Key Milestones/ Future Activities .....	27
CHAPTER 4 – EXPECTED RESULTS .....		27
CHAPTER 5 – RESULTS AND DISCUSSION .....		29
5.1	Permeability Test Using PoroPerm.....	29
5.2	Simulation of Various Field Data Using Laboratory Permeability Results.	31
5.2.1	Gas Production Rate Curve and Water Production Rate Curve.....	32
5.2.2	Total Gas Production Curve and Total Water Production Curve .....	33
5.3	Comparison of Simulation Results to Powder River Basin .....	34
5.4	Relationship between Stress Changes and Permeability .....	36
CHAPTER 6 – CONCLUSIONS AND RECOMMENDATIONS .....		38
6.1	Conclusion .....	38
6.2	Recommendations.....	38
Nomenclature .....		39
Bibliography.....		41

## Table of Figures

Figure 1 Coalification process of organic debris as a function of time, pressure and heat .....	5
Figure 2 Process of coalification.....	6
Figure 3 Properties of different coal rank .....	7
Figure 4 Plane view of coal cleat orientations .....	8
Figure 5 Cross section of coal cleat orientation .....	8
Figure 6 Dual porosity characteristics of coal.....	9
Figure 7 Relationship between Langmuir volume and pressure .....	10
Figure 8 Relationship between Langmuir volume and Langmuir pressure .....	10
Figure 9 Three Stages of Coalbed Methane Production .....	11
Figure 10 Changes in relative permeability in coal during production stages .....	12
Figure 11 Matchstick fracture system.....	14
Figure 12 Idealization of dual porosity model of heterogeneous reservoir .....	16
Figure 13 Schematic diagram of experimental setup to measure bulk and pore compressibility .....	18
Figure 14 Schematic diagram of triaxial loading acting on coal sample .....	19
Figure 15 Experiment setup to measure matrix compressibility and matrix shrinkage compressibility .....	20
Figure 16 Sorption capacity of nitrogen, carbon dioxide and methane gases.....	21
Figure 17 PoroPerm in Universiti Teknologi PETRONAS .....	22
Figure 18 Schematic of gas permeameter in PoroPerm device.....	24
Figure 19 Point Load Tester .....	25
Figure 20 Flow Chart for Final Year Project .....	26
Figure 21 Final Year Project Gantt Chart with Key Milestones and Future Activities .....	27
Figure 22 Expected results of effects of compressibilities on gas production rate .....	28
Figure 23 Comparison of maximum permeability for different coal fields .....	30
Figure 24 Simulated gas and water production rate curve of Sarawak coal field.....	32
Figure 25 Simulated cumulative water and gas production curve of Sarawak coal field ....	33
Figure 26 Simulated GIIP of Sarawak coalfield .....	33
Figure 27 Comparison of Gas Production Rate of Sarawak Coal Field and Powder River Basin .....	35
Figure 28 Load vs Permeability .....	37

## Table of Tables

Table 1 Classification of permeability values with respect to coal field production quality .	29
Table 2 Permeability result of Sarawak coal samples.....	29
Table 3 Input data for predicting Sarawak coal field CBM production.....	31
Table 4 Coal Properties of Powder River Basin .....	35
Table 5 Single Point Load Testing Results .....	36



# CHAPTER 1

## INTRODUCTION

### 1.1 Background of Study

As the reserve of conventional hydrocarbon dwindles, coupled by the fact that there is an increasing need of energy, the energy industry has shifted its focus into unconventional hydrocarbon sources. Coalbed methane (CBM) is one of the sources of unconventional hydrocarbon (Australia Science Media Center, 2012).

CBM is found and stored in layers of coalbed. During the coalification process, gases such as methane, ethane, nitrogen, carbon dioxide, etc are produced. Methane is usually the dominant gas in terms of volume. These gases are stored in the coalbed in two ways. Firstly, these gases can be found as free gases in the natural porosity of the coal. Secondly, these gases are adsorbed to the surface of the coal due to the aquifer pressure acting on the coalbed (Dunn, 1989). During the production of natural gases from the coalbed, reservoir pressure decreases as the aquifer water is being produced to the surface (dewatering). When the desorption point is achieved, which is the pressure at which natural gas begins to desorb from the surface of the coal, natural gas will be produced together with the remaining aquifer in a two-phase flow (Irawan et al, 2012).

During the production stage of coalbed methane, compressibility of the coal undergoes changes due to the change in effective stress surrounding the coal as well as the sorption of gases from the coal matrices. Compressibility of coal can be looked from several aspects, namely bulk compressibility, pore compressibility, matrix compressibility and matrix shrinkage compressibility. Experiments in the past showed that gas permeability in coal is highly stress-dependent. Gas permeability in coal is expected to be reduced if effective stresses surrounding the coal increases, as the macropore channel decreases in size due to stresses acting on the coal. Meanwhile, sorption induced swelling and shrinkage also affects the gas permeability of coal, with shrinkage of coal matrix causing increase in gas permeability and vice versa (Jasinge et al, 2010).

## **1.2 Problem Statement**

### **1.2.1 Problem Identification**

When the reservoir pressure in a coalfield is declining during the production stage, coal solids and their pore spaces will experience volumetric and geometrical changes. Different compressibility of coal, i.e. bulk, matrix, pore volume and matrix shrinkage, has its own unique influence on the coal's permeability, and subsequently the production of natural gases from the field. Hence, careful study has to be carried out on the matrix properties of coal in order to maximize or optimize the production of CBM.

### **1.2.2 Significance of the Project**

Through this project, coal samples from Sarawak, Malaysia will be experimented in laboratory to determine the effect of its compressibility towards its permeability. After that, software simulation study is carried out to provide an estimation of the natural gas production potential based on the value of permeability obtained. As Malaysia has yet to have a proven CBM reserves, the simulation study of Malaysian coal is compared to CBM producing fields in U.S.(Powder River Basin and San Juan Basin) to relate the impact of compressibility and permeability for optimized CBM production.

## **1.3 Objectives**

The objectives of this research are:

- i. To carry out laboratory experiment to ascertain the effect of coal compressibility towards its permeability
- ii. To carry out software simulation that estimates the potential natural gas production based on the different values of compressibility to optimize CBM production
- iii. To compare the potential of Malaysian coal to be CBM producing fields with other producing CBM fields, namely Powder River Basin, U.S.

#### **1.4 Scope of Study**

The scope of this study involves the petrology of coal and reservoir engineering of CBM. Using the coal samples from coalfield in Sarawak gives a greater insight into the matrix properties and flow behaviours affected by different compressibility values of Malaysian coal.

#### **1.5 Relevancy of the Project**

By investigating the effect of coal compressibility towards its permeability, a better understanding of the flow behaviour of CBM reservoir and its production can be obtained. This knowledge will be useful in optimizing CBM production from a given field. Besides that, the declining of conventional hydrocarbon has led to a more active pursuit of unconventional hydrocarbon such as CBM. As a matter of fact, CBM is a known cheaper alternative to oil or coal (solid matrix) as a source of energy, and less harmful to the environment. Thus, the study on CBM will be invaluable for the future of harnessing energy.

#### **1.6 Feasibility of the Project within the Scope and Time Frame**

In order for the project to be feasible, three important aspects have to be looked into:

i. Time

This project is divided into two major sections, namely Final Year Project I (FYP I) and Final Year Project II (FYP II), spanning two academic semesters. In FYP I, the scope of work covered included background of study, literature review and methodology. In FYP II, the scope of work included carrying out laboratory experiments of coal compressibility, software simulation of CBM production and analysing all the results obtained. Through a proper segregation of tasks involving FYP I and FYP II, the time allotted was sufficient for the completion of this project.

ii. Laboratory equipment and samples

All the laboratory equipment needed to investigate the effects of coal compressibility towards its permeability was available in the Universiti Teknologi PETRONAS (UTP) laboratory. The equipment was still functioning properly and they were correctly calibrated to avoid any systemic error to obtain greater accuracy and consistency in results. Samples used in this laboratory experiment were coal samples taken from Sarawak, Malaysia. These samples were readily available in UTP as previous researches carried out required tests done on these samples.

iii. Software simulations

Software simulations used in estimating the CBM productions included Eclipse CBM. Eclipse CBM (Schlumberger) was readily available in UTP via various collaborations between the software owners and the university.

iv. Literature resources

The literature resources used to complete this project consisted of Society of Petroleum Engineers (SPE) technical papers, journal articles, conference proceedings, textbooks and previous FYP thesis. These resources could be easily obtained via various sources such as [www.onepetro.org](http://www.onepetro.org), Information Resource Center (IRC-UTP), [www.utpedia.edu.my](http://www.utpedia.edu.my), Journal of Petroleum Technology (JPT), etc.

## CHAPTER 2

### LITERATURE REVIEW

#### 2.1 Formation of Coal

Coal is a type of sedimentary rock that forms from the accumulation and compaction of plant remains deposited at swamps which created peat. Continuous deposition of plant-derived organic material in a deoxygenated environment inhibits microorganisms such as fungi or bacteria from decomposing these plant materials, thus, allowing it to be continuously accumulated, preserved and buried. This process is called peatification (Rogers et al, 2007) (Strickland et al, 2008).

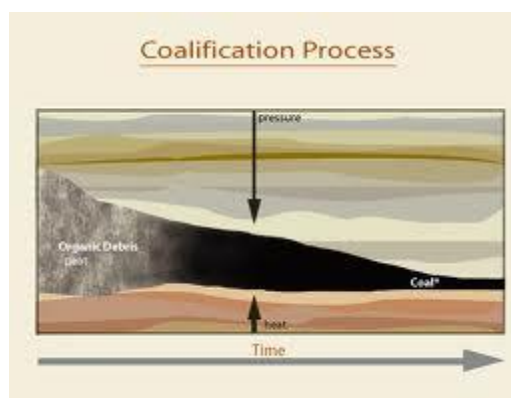


**Figure 1 Coalification process of organic debris as a function of time, pressure and heat (Alberta Energy, 2013)**

Next, these peats are converted into coal in a process called coalification. Coalification can be categorized into two distinct processes, namely biochemical degradation and geochemical degradation. During the biogenic stage of coalification, methane is produced from the breakdown of plant materials by aerobic and anaerobic bacteria. However, due to the limited oxygen content in a peat environment, these plant materials were not completely broken down by the bacteria. As such, the remaining plant matrices that were not broken down would then undergo thermogenic degradation as a function of time, overburden pressure and subsurface temperature to be converted into coal (Anderson, 2003).

## 2.2 Coal Rank

Coal rank is a measure of maturity as to how much coalification that has been undergone from peat to anthracite. Coals can be categorized into several stages, which may include (in order of increasing rank): peat, lignite, subbituminous, bituminous and anthracite(Australian Coal Association Research Program, 2013).

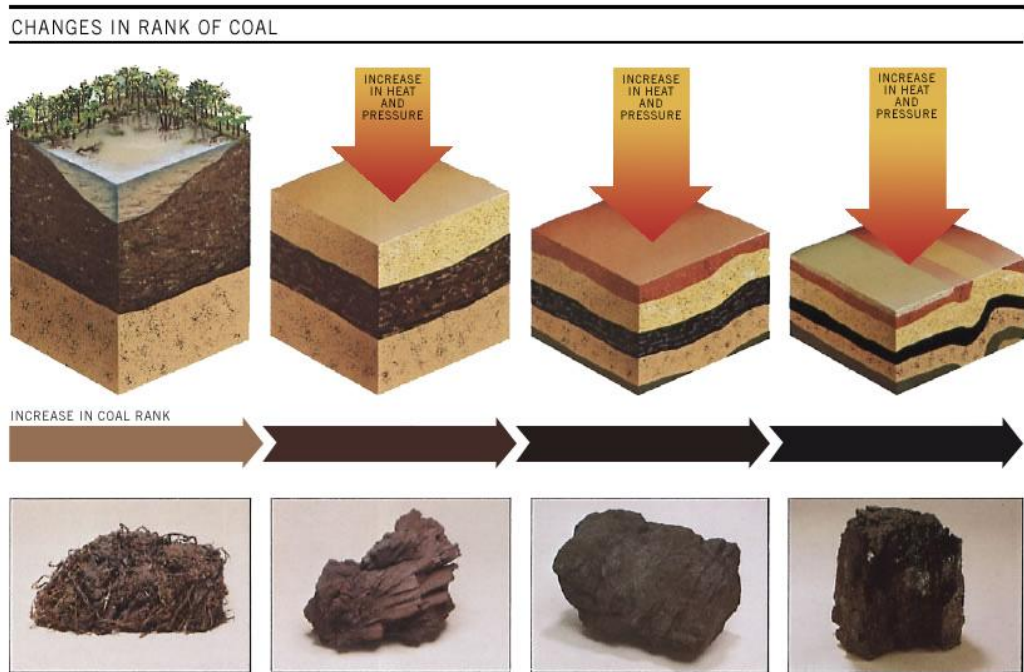


**Figure 2 Process of coalification (Australian Coal Association Research Program, 2013)**

COAL RANK	CARBON CONTENT (%)	VOLATILE MATTER (%)	CALORIFIC VALUE (kJ/kg)	MOISTURE CONTENT (%)
PEAT	60	>53	16800	>75
BROWN COAL	60 – 71	53 – 49	23000	35
SUB-BITUMINOUS COAL	71 – 77	49 – 42	29300	25 – 10
BITUMINOUS COAL	77 – 87	42 – 29	36250	8
ANTHRACITE	77 – 87	29 – 8	>36250	<8
-	On dry ash free basis	On dry ash free basis	Ash free basis	In-situ

**Figure 3 Properties of different coal rank (Australian Coal Association Research Program, 2013)**

### 2.3 Dual Porosity Characteristic of Coal Structure

Unlike conventional reservoir rocks, coal is distinguished by its dual-porosity characteristic which consists of micropore and macropore system (Aminian, 2007). Macropore system refers to the coal cleats, which are natural opening fractures in coal beds. Cleats commonly exist in two sets, namely butt cleats and face cleats. Face cleats are usually formed first in the formation of coal rocks, and they are continuous; On the other hand, butt cleats are formed after face cleats and they formed in between two parallel adjacent face cleats (Laubach, Marrett, Olson, & Scott, 1997). These two sets of cleats exist mutually perpendicular to one another, and together, they are perpendicular to the coal bedding. Even though cleat porosity only stands at 0.5% to 2.5% of the coal total porosity and only small amount of free methane gas exists in it, understanding of cleat system is still important in optimizing production of coalbed methane (Puri, Evanoff, & Brugler, 1991). This is because gas desorbed from the surface of coal micropore must diffuse through the coal matrix until a network of open fracture, i.e. cleat system is encountered. The permeability in cleat system creates the flow path for desorbed gases to flow to the producing wellbore, thus, making it critical to the amount of gas that can be produced (Laubach et al, 1997).

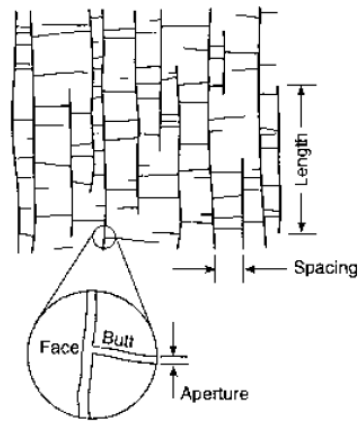


**Figure 4 Plane view of coal cleat orientations (Laubach & Tremain, 1991)**

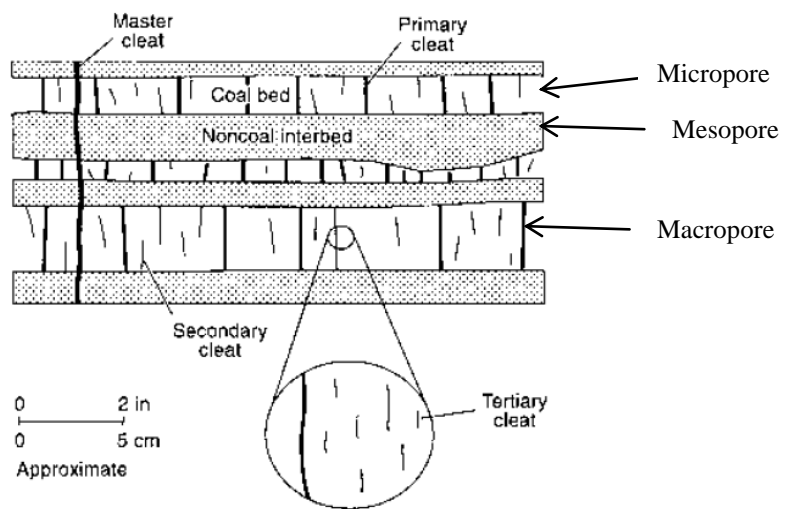


**Figure 5 Cross section of coal cleat orientation (Laubach & Tremain, 1991)**

Micropore system of the coal matrix acts as the primary site for the adsorption of gases in the coal. These micropores are located within the matrix of the coal and measures approximately 5 – 10 Angstrom(Fekete Associates Inc., 2011). Gas is stored on the surface of the coal within the micropores of the matrix, existing as a single layer of molecules in a condensed, near-liquid state. This internal surface area of the coal is so large that even a single adsorbed layer of molecules constitutes a significant quantity of gas. Hence, 98% of gas volume in coal is actually stored in its micropore system(Gray, 1987).

Despite its dual-porosity characteristics, a third natural fracture, namely mesopore, actually exists in coal, which is its bedding plane. Bedding plane refers to the horizontal gap that exists between different layers of coal. However, bedding plane is usually insignificant towards flow of gases in coal due to the overburden pressure acting on it(Harpalani S. , 1999).



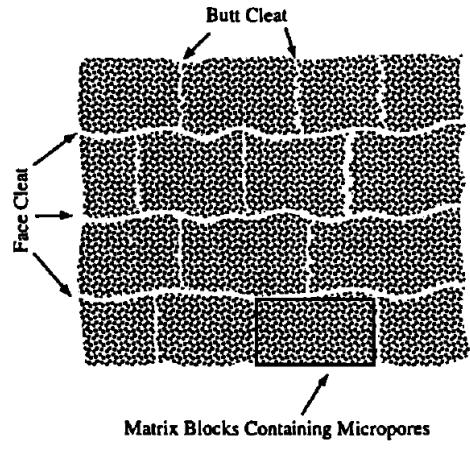


**Figure 6 Dual porosity characteristics of coal (Harpalani S. , 1999)**

**2.4 Gas Storage and Transportation in Coal**

As described earlier, gases stored in coal can exist either as free gas molecules in the macropore system or as gas molecules adsorbed on the surface of its micropore system. The free gas in the macropore system can be calculated using the following formula (Fekete Associates Inc., 2011):

$$Q = \frac{\Phi Ah (1 - S_w)}{B_g}$$

**Equation 1**

Gas transportation in the macropore system will adhere to the Darcy Law, just as the conventional reservoir does. However, the storage and and transportation of gas in micropore system of coal is of the interest for most researchers due to the adsorptive nature of the micropore system.

The adsorption and desorption of gas, simply known as gas sorption, is the physical movement of gas across the coal micropore surface layers which depends on the methane concentration gradient as a driving force. A weak van der Waals force exists between gas molecules and coal micropore surface layers which holds the gas molecules to the coal surface. Adsorption should not be confused to absorption, which is a physical process in which a substance is trapped within another substance. Due to the nature of the van der Waals forces involved in adsorption of gases onto coal layers, this process is easily reversible once the coal has been dewatered during the production phase of coalbed methane (Moffat & Weale, 1955).

The Langmuir Adsorption Isotherm adequately describes the relationship between the quantity of gas adsorbed in coal at different pressure and temperature.

Langmuir equation is shown below(Langmuir, 1918):

$$Q = \frac{V_L P}{P_L + P}$$

**Equation 2**

The two main parameters in the above formula are Langmuir Volume Parameter,  $V_L$ , and Langmuir Pressure Parameter,  $P_L$ .  $V_L$  refers to the maximum quantity of gas adsorbed on a coal matrix and infinite pressure.  $P_L$  refers to the pressure at which the half of the monolayer capacity of the coal surface has been occupied with gases.

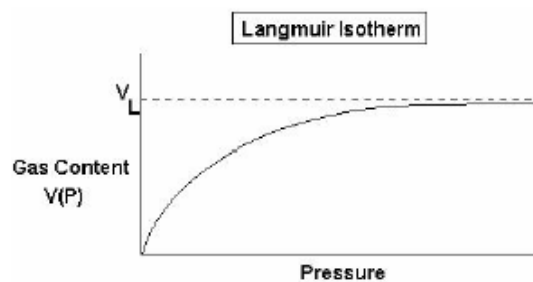


**Figure 7 Relationship between Langmuir volume and pressure (Fekete Associates Inc., 2011)**

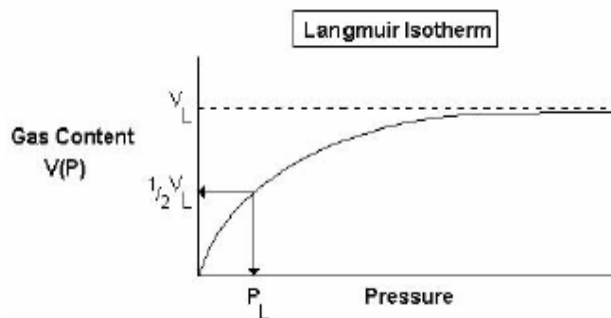


**Figure 8 Relationship between Langmuir volume and Langmuir pressure (Fekete Associates Inc., 2011)**

In its natural form, the natural cleat of coal is typically water saturated. This creates a hydrostatic pressure in which the gas in coal is kept adsorbed on the coal surfaces by this pressure. During the early production life of a coalbed methane well, this water must be removed from the coal in a process called

dewatering. The removal of the hydrostatic pressure brings about desorption of gas from the coal surface. Desorbed gas will then flow into the coal cleat, creating a concentration gradient at the interface between coal cleat and surface layer. Movement of the gas from the coal surface layer to the cleat follows the Fick's Law, as shown below:

$$M = D\Delta C$$

*Equation 3*

After the gas has been diffused out to the coal cleat, the movement of gas in the cleat obeys Darcy Law as shown below:

$$M = \frac{\rho k}{\mu} \Delta P$$

*Equation 4*

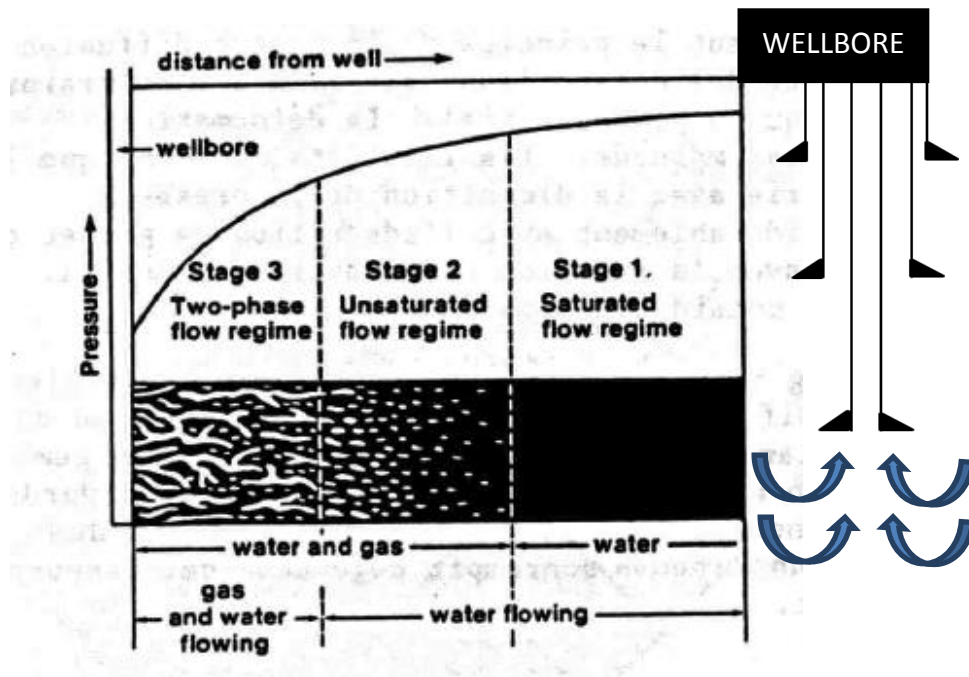


**Figure 9 Three Stages of Coalbed Methane Production (Modified from Harpalani et al 1991)**

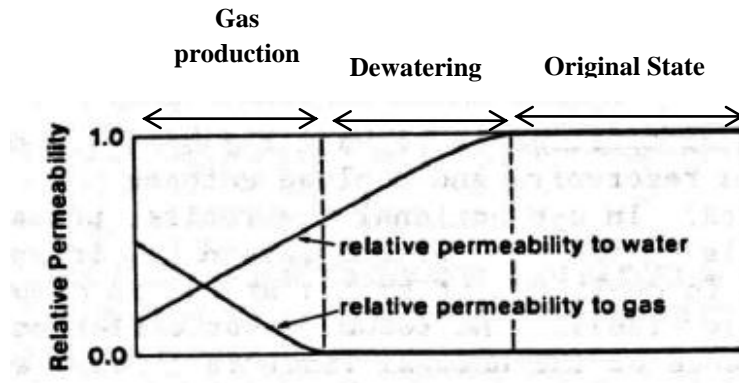


**Figure 10 Changes in relative permeability in coal during production stages  
(Harpalani, Zhao, & Farmer, 1991)**

**2.5 Bulk Compressibility, Pore Volume Compressibility, Matrix Compressibility, Matrix Shrinkage Compressibility and Permeability Model of Coal**

Compressibility describes the relationship between the volume and the pressure exerted on a body. Given that coal is exerted by both external pressure (overburden and hydrostatic) and internal pressure (pore pressure), it is imperative to consider different types of compressibility acting on it.

**2.5.1 Bulk Compressibility**

Bulk volume,  $V_b$ , refers to the volume of the coal without its pore spaces. Hence, bulk compressibility,  $C_b$ , refers to the fractional change in bulk volume per unit change in external pressure when internal pressure is held constant, as shown below (Harpalani S. , 1999):

$$C_b = \frac{1}{V_b} \cdot \frac{dV_b}{dP_e}$$

**Equation 5**

### 2.5.2 Pore Compressibility

Pore volume,  $V_p$ , refers to the volume of the pore spaces in the coal. Hence, pore compressibility,  $V_p$ , refers to the fractional change in pore volume per unit change in internal pressure when external pressure is held constant, as shown below (Harpalani S. , 1999):

$$C_p = \frac{1}{V_p} \cdot \frac{dV_p}{dP_i}$$

*Equation 6*

### 2.5.3 Matrix Compressibility

Matrix compressibility refers to the fractional change in volume of coal solid material per unit change in both internal and external pressure, as shown below (Harpalani S. , 1999):

$$C_m = \frac{1}{V_m} \cdot \frac{dV_m}{dP}$$

*Equation 7*

### 2.5.4 Matrix Shrinkage Compressibility

When gas desorbs from the surface of the coal, matrix of the coal will undergo shrinkage (Gregg, 1961). Hence, matrix shrinkage compressibility refers to the fractional change in matrix volume per unit change in pressure of a sorbing gas, as shown below (Harpalani S. , 1999):

$$C_{ms} = \frac{1}{V_m} \cdot \frac{dV_m}{dP_s}$$

*Equation 8*

### 2.5.6 Matchstick Permeability Model for Coal

Seidle et al formulated a theory of modeling stressed coalbeds to a naturally fractured reservoir geometry in the form of a collection of matchsticks. This theory was tested against laboratory experiments using samples from San Juan Basin and Warrior Basins to good agreement in terms of laboratory data and theoretical behavior (Seidle, Jeansonne, & Erickson, 1995).

If a coal matrix is compared to a matchstick fracture system, with the cleats having homogenous and smooth plane channels, porosity and permeability models can be derived.

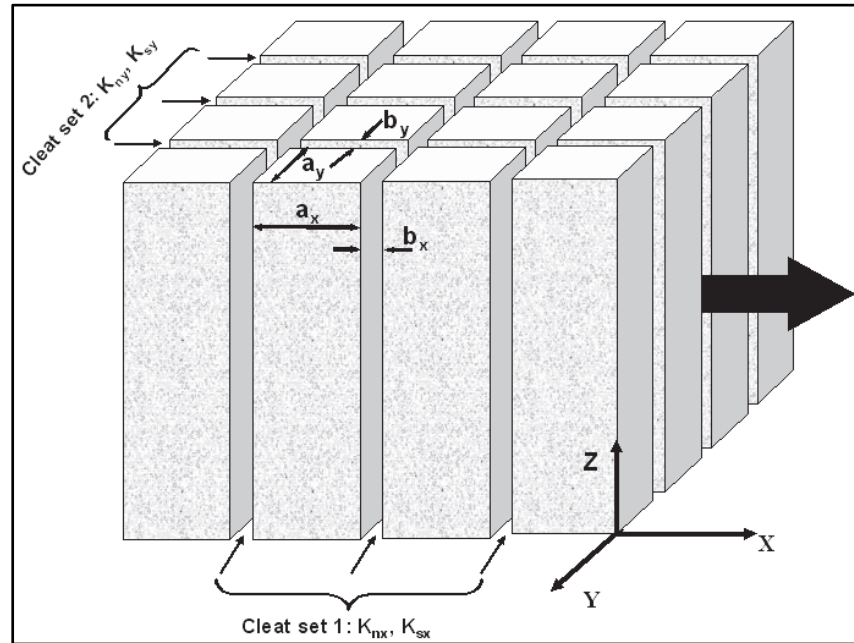


**Figure 11 Matchstick fracture system (Gu & Chalaturnyk, 2006)**

Without considering any changes in pressure or swelling/shrinkage on the coal, equations for porosity and permeability can be obtained as follows (Van Golf-Racht, 1982):

$$\phi = \frac{2b}{a}$$

**Equation 9**

$$k = \frac{1}{24} b^2 \phi$$

**Equation 10**

During ‘dewaterating’ stage, coalbeds undergo pressure changes as hydrostatic pressure is reduced, resulting in increment of net overburden stress. In such instances, equation for permeability can be obtained as follows (Seidle et al, 1995):

$$\frac{k}{k_o} = \frac{e^{-3c_p \Delta \sigma}}{1 - \phi_o(1 - e^{-c_p \Delta \sigma})}$$

**Equation 11**

When considering matrix shrinkage or swelling due to sorption, porosity changes can be modeled as follows:

$$\frac{\phi}{\phi_o} = 1 + \left(1 + \frac{2}{\phi_o}\right) c_m v_m \left(\frac{b' p_o}{1 + b' p_o} - \frac{b' p}{1 + b' p}\right)$$

**Equation 12**

After obtaining the porosity value under swelling/shrinkage effect, the permeability can once again be calculated using Equation 10.

The limitation of matchstick permeability of coal by Seidle et al. has been discussed by Palmer & Mansoori (1995). Palmer & Mansoori argues that matchstick model is based on triaxial-stressed core samples experimented in the lab and does not entirely represent the actual uniaxial-stress induced to the coalbed in actual reservoir.

**2.5.7 Numerical Simulation of CBM with Eclipse**

Eclipse CBM model by Schlumberger are three-dimensional, dual-phase and able to model the CBM production. However, a limitation of this model is that it is not able to consider the changes in fracture porosity and permeability brought upon by matrix shrinkage and swelling during coal sorption. The model used in Eclipse is formulated from Warren and Root for conventional naturally fractured reservoir and treated matrix sorption as a pseudosteady-state transport process(Wei et al, 2006). The original Warren and Root model will not be discussed explicitly in this section and reference can be made to the original paper published by the said author.

Eclipse CBM model consists of two interconnected systems representing the coal matrix and the permeable rock fractures. To model such systems, two simulation cells are associated with each block in the geometric grid, representing the coal matrix and fracture

volumes of the cell. In contrast to the oil dual porosity model, only the gas concentration is of concern in the coal matrix system of coal dual porosity model. In the natural fracture system, i.e. cleat, the natural flow model is utilized(Schlumberger, 2008).

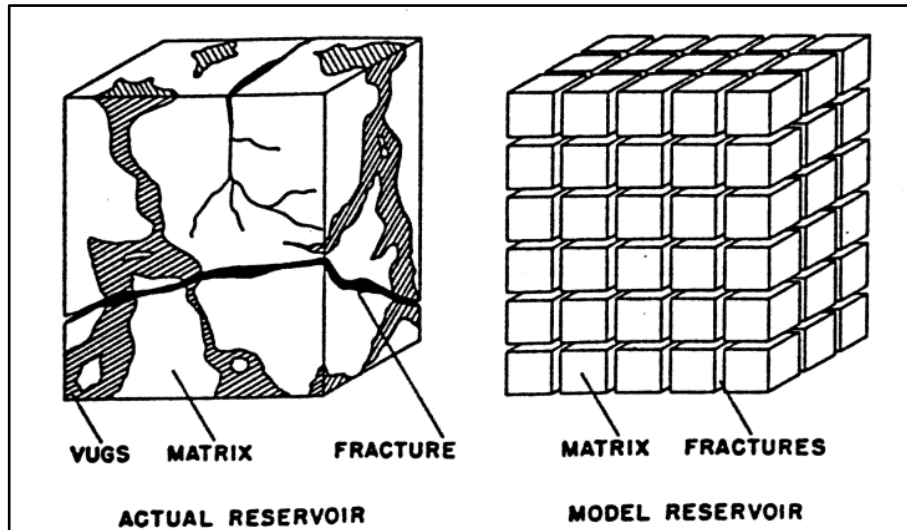


**Figure 12 Idealization of dual porosity model of heterogeneous reservoir (Warren & Root, 1963)**

Each block in the interconnected system can be defined independently. The pore volume of the fracture system represents the non-coal volume of a simulation cell. If the pore volume is designated as  $\phi$ , the coal volume in a unit simulation cell is given as  $1-\phi$ . Assuming  $\Omega$  as the bulk volume of the simulation cell, the coal volume within the total cell is given as(Stopa & Nawrat, 2012):

$$W_c = (1-\phi)\Omega$$

**Equation 13**

Volume of gas adsorbed in the simulated cell is given as  $(1-\phi)\Omega\rho_c V$ , where  $V$  is actual volume of gas adsorbed per unit mass of a coal and  $\rho_c$  is the coal density.

When the fractured porosity is altered, the cell porosity can be calculated as shown below(Stopa & Nawrat, 2012):



$$\Delta\phi = \frac{\Delta Q_c}{\rho_c \Omega}$$

**Equation 14**

The notation  $\Delta Q_c$  represents the mass of coal removed from a simulation cell that corresponds to the volume of altered porosity. This mass of coal removed will be replaced by additional volume of gas released from the coal removed. The total flow of gas from the coal matrix to the fractures within a simulation cell is given as follow (Stopa & Nawrat, 2012):

$$q_{mf} = D\sigma(V - V_E)[(1 - \phi)\Omega\rho_c - \Delta Q_c] + V \cdot \frac{\Delta Q_c}{\Delta t}$$

**Equation 15**

$\sigma$  represents the factor to account for the matrix-fracture interface area per unit volume and  $D$  is the diffusion coefficient while  $V_e$  is the Langmuir volume equilibrium. Equation 15 is a rough estimation model as to how Eclipse CBM obtains the production volume in a coalbed reservoir simulation and modelling (Stopa & Nawrat, 2012).

It has to be noted that accurate estimation of CBM production based on simulator is difficult due to the multiple aspects affecting the gas reservoirs in coalbed.

In the case of Eclipse CBM simulator, time dependent parameters such as changes in permeability and porosity during matrix shrinkage and swelling cannot be accounted for in this simulator. The method to overcome this is by predicting the porosity and permeability of the coal throughout its production life cycle and input them into the simulator.

Secondly, the Eclipse CBM model is formulated from Warren and Root model for naturally fractured conventional reservoir. However, it is well understood that CBM is not a conventional reservoir as its coal matrix undergo swelling and shrinkage during the production

cycle. Notwithstanding, Warren and Root model is currently the closest model there is to simulate the coalbed reservoirs and this model is widely adopted by many other simulators.

The sorption of gases in coalbed reservoirs is also a subject of continuous study at the moment. As stated earlier, sorption is defined by Fick's Law, which is the diffusion of gases due to concentration gradient. However, in actual fact, there are many other factors that can affect sorption of gases, such as heat, temperature, pressure to name a few. These other factors are not considered in Fick's Law, and thus, affecting the accuracy of Eclipse CBM simulators.

## 2.6 Previous Laboratory Studies on Compressibility

### 2.6.1 Bulk and Pore Compressibility

Measurement of bulk and pore compressibility under triaxial stress conditions can be carried as shown in the schematic below:

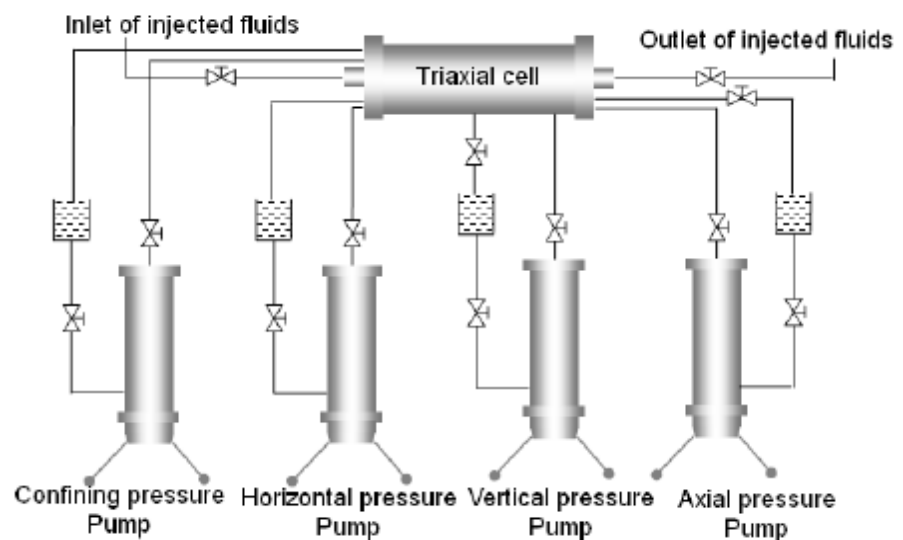


**Figure 13 Schematic diagram of experimental setup to measure bulk and pore compressibility (Zeng, Xua, Heb, & Wang, 2011)**

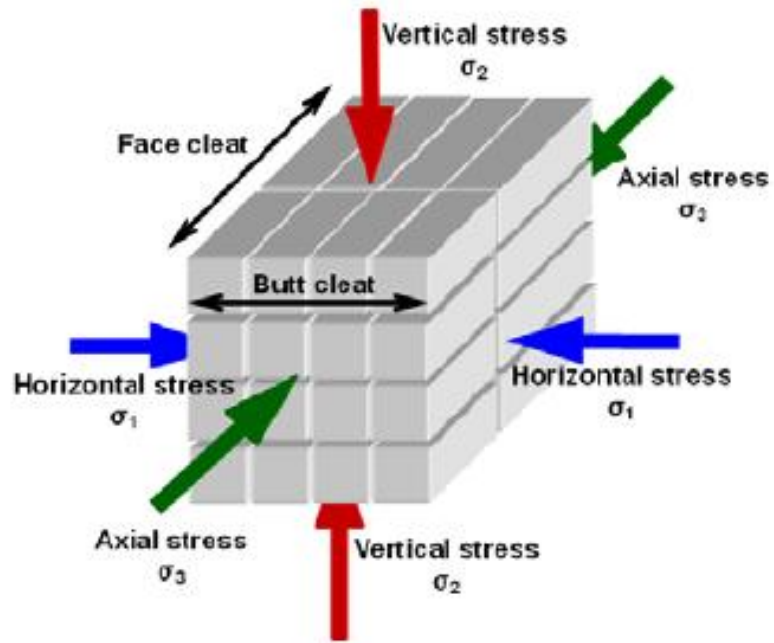


**Figure 14 Schematic diagram of triaxial loading acting on coal sample (Zeng, Xua, Heb, & Wang, 2011)**

To obtain the bulk compressibility, the stress acting on the sample is increased gradually until a graph of change of volume,  $\Delta V$ , vs stress is obtained. Bulk compressibility can be determined from the relationship of  $\Delta V$  vs stress.

To obtain the pore compressibility, external pressure will be kept constant while gas pressure in the sample is increased gradually until a graph of a change in volume,  $\Delta V$ , vs pressure is obtained. Pore compressibility can be determined from the relationship of  $\Delta V$  vs pressure.

### **2.6.2 Matrix and Matrix Shrinkage Compressibility**

Measurement of matrix and matrix shrinkage compressibility can be carried out as shown in the diagram below:

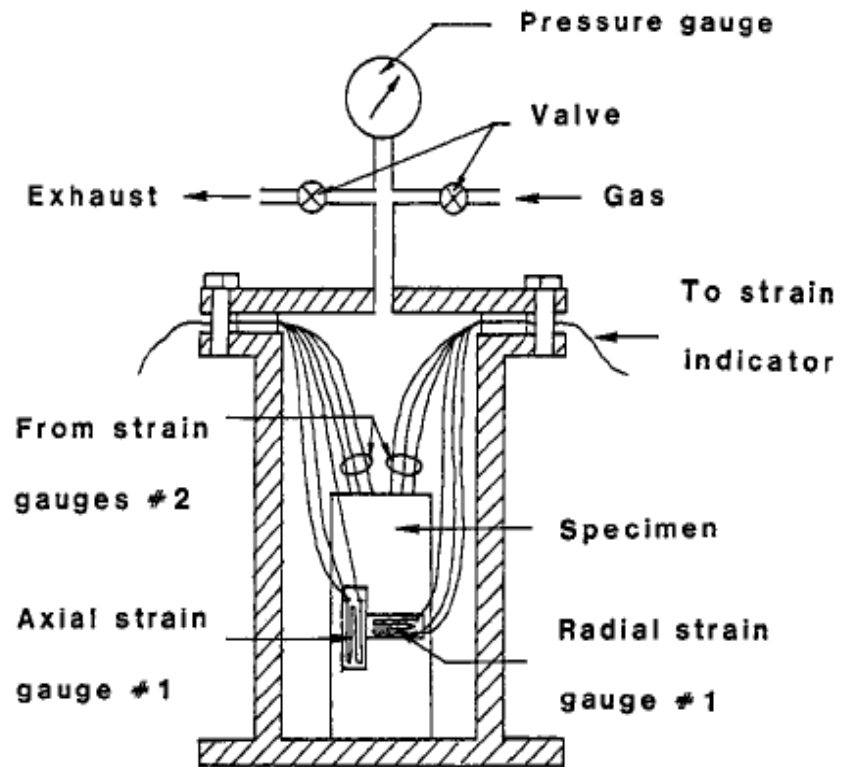


**Figure 15 Experiment setup to measure matrix compressibility and matrix shrinkage compressibility (Harpalani & Schraufnagel, 1990)**

Matrix compressibility and matrix shrinkage compressibility can be obtained through the strain measurement of different concentration of methane-helium gas of equal pressure.

### **2.6.3 Laboratory Study of Sorption Capacity of Various Gases**

Reeves et al employed a simple uni-variate analysis and obtain results that indicate that CH<sub>4</sub> and N<sub>2</sub> sorptive capacity increases with coal rank in a statistically meaningful fashion. However, no such trend exists for CO<sub>2</sub>. If a relationship does exist between coal rank and CO<sub>2</sub> sorptive capacity, it must be influenced by other factors not accounted for in this simple model.

The model also shows that carbon dioxide has the highest sorption capacity in coal when compared to methane, and followed lastly by nitrogen. This corroborates with the industrial practice of using

carbon dioxide for the degasification of methane from coalbed reservoirs(Reeves et al., 2005).

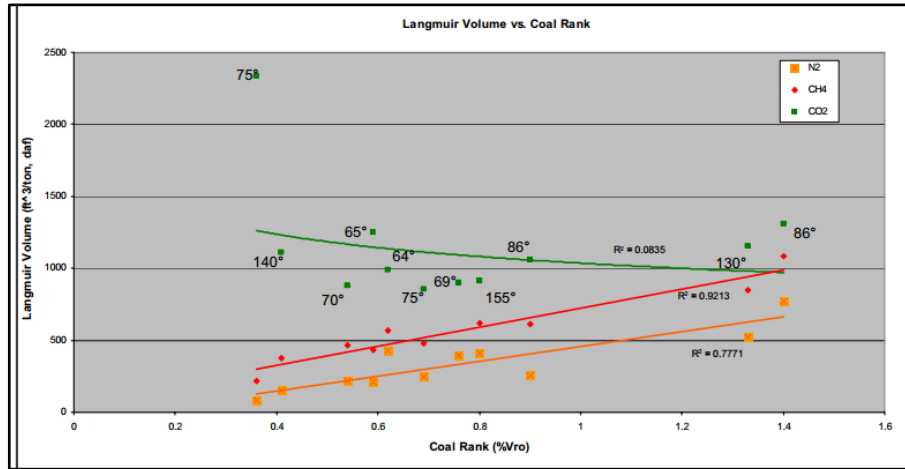


**Figure 16 Sorption capacity of nitrogen, carbon dioxide and methane gases(Reeves et al., 2005)**

## CHAPTER 3

### METHODOLOGY

#### 3.1 Laboratory Study of Permeability Using PoroPerm

##### 3.1.1 Objective of Permeability Study Using PoroPerm

Objective of laboratory study using PoroPerm in this research is to determine the permeability of the coal samples under API condition. The main equipment that will be used is PoroPerm, which is available in Block 15, Petroleum Engineering Department, Universiti Teknologi PETRONAS.



**Figure 17 PoroPerm in Universiti Teknologi PETRONAS**

##### 3.1.2 Sample Description and Preparation

Core samples of bituminous coal from Balingian coal field, Mukah, Sarawak were obtained for the purpose of this experiment. These samples were stored under room conditions and all the methane gases previously stored in the coal have been desorbed.

For preparation of the permeability test using PoroPerm, a core plug measuring 3 inch x 1.5 inch were bored out from the coal samples.

### **3.1.3 Experimental Procedures**

The procedure adopted for permeability study using PoroPerm device consists of the coal core plug being mounted in the pressure chamber. The chamber is then sealed tightly and pressurized to a predetermined API condition and maintained constant at that temperature and pressure rating. A substitute for methane gas is used due to the combustible nature of methane gas, which due to safety concern, will not be flowed through the core plug. Instead, nitrogen and carbon dioxide gases will be flown through to permeate the core plug. Adsorption capacity of coal relative to nitrogen, carbon dioxide and methane has been discussed and accounted for in the earlier section in literature review (section 2.6.3).

Transient measurements employ fixed-volume reservoirs for gas. These may located upstream of the sample from which the gas flows into the sample being measured. The pressure falloff apparatus (Figure 17) employs an upstream gas manifold that is attached to a core plug holder capable of applying hydrostatic stresses to the core plug of diameter 1.5” and length 3”. An upstream gas reservoir of calibrated volume can be connected to the calibrated manifold volume by means of a valve.

The downstream end of the sample is vented to atmospheric pressure. An accurate pressure transducer is connected to the manifold immediately upstream of the sample holder. The reservoir, manifold and sample are filled with gas.

After a few seconds for thermal equilibrium, the outlet valve is opened to initiate the pressure transient. When the upstream pressure has decayed to about 85% of the fill pressure, data collection is started. Pressures and times are recorded.

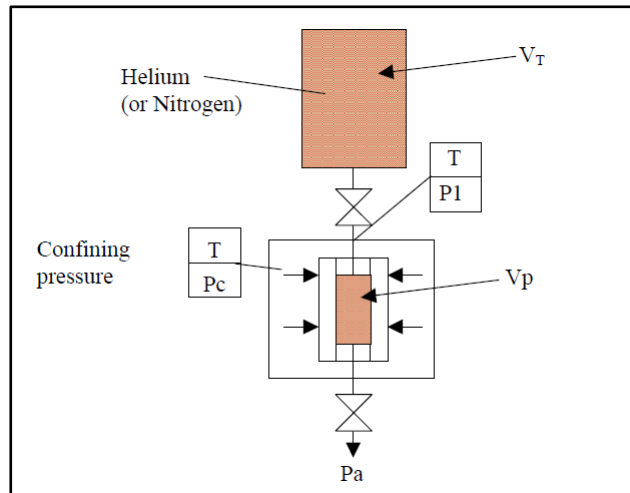


**Figure 18 Schematic of gas permeameter in PoroPerm device**

## **3.2 Laboratory Study of Compressibility Using Point Load Test**

### **3.2.1 Objective of Compressibility Study Using Point Load Test**

Objective of laboratory study using Point Load Test in this research is to determine the maximum load of the coal samples under compression or stressed condition. The main equipment that will be used is Point Load Tester, which is available in Block 14, Petroleum Geoscience Department, Universiti Teknologi PETRONAS.

### **3.2.2 Sample Description and Preparation**

Same core samples of bituminous coal from Balingian coal field, Mukah, Sarawak were obtained for the purpose of this experiment. These samples were stored under room conditions and all the methane gases previously stored in the coal have been desorbed.

For preparation of the permeability test using triaxial cell, five rectangular sample measuring 70mm (length) x 50mm (width) x 30mm (height) were bored out from the coal samples.

### **3.2.3 Experimental Procedures**

For the point load test, the confining pressure is provided by mineral oil. The core plug is inserted into the cell. The PLT involves the



compressing of a rock sample between conical steel plates until failure occurs. The apparatus for this test consists of a rigid frame, two point load platens, a hydraulically activated ram with pressure gauge and a device for measuring the distance between the loading points. The pressure gauge should be of the type in which the failure pressure can be recorded.

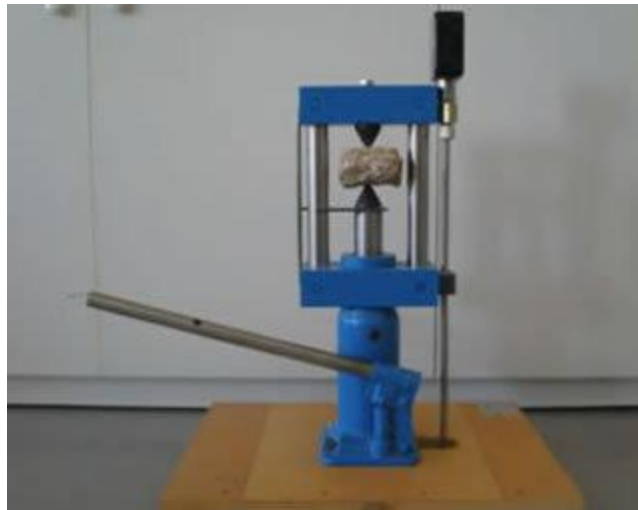


**Figure 19**Point Load Tester

### **3.3 Software Simulation Study**

Software simulation study will be carried out to determine the production of the Malaysian coal samples under different compressibility values. This simulation will be carried out using Eclipse CBM from Schlumberger. The model used by Eclipse has been discussed extensively earlier in literature review section, which includes the model adopted and the limitation of its application (section 2.5.7).

### 3.4 Flow Chart

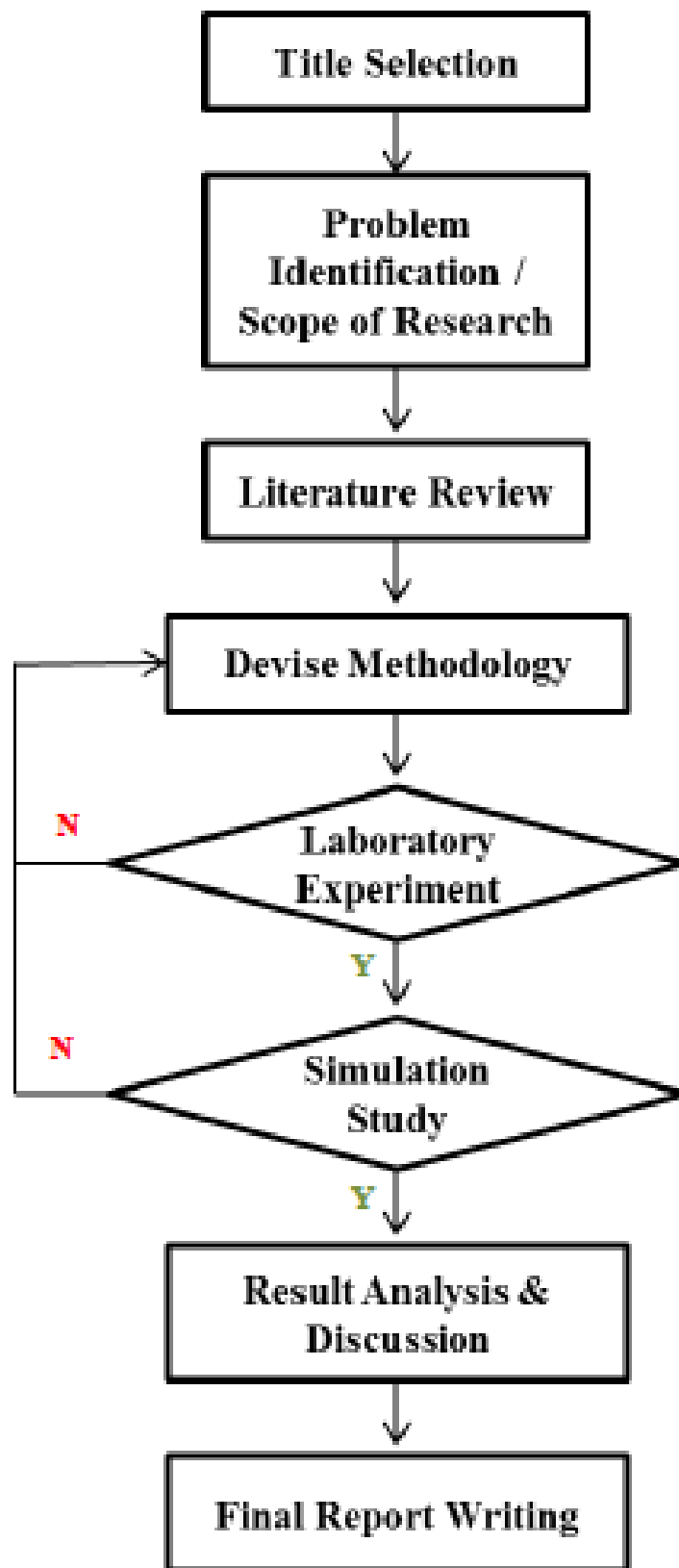


Figure 20 Flow Chart for Final Year Project

### 3.5 Project Timeline/ Key Milestones/ Future Activities

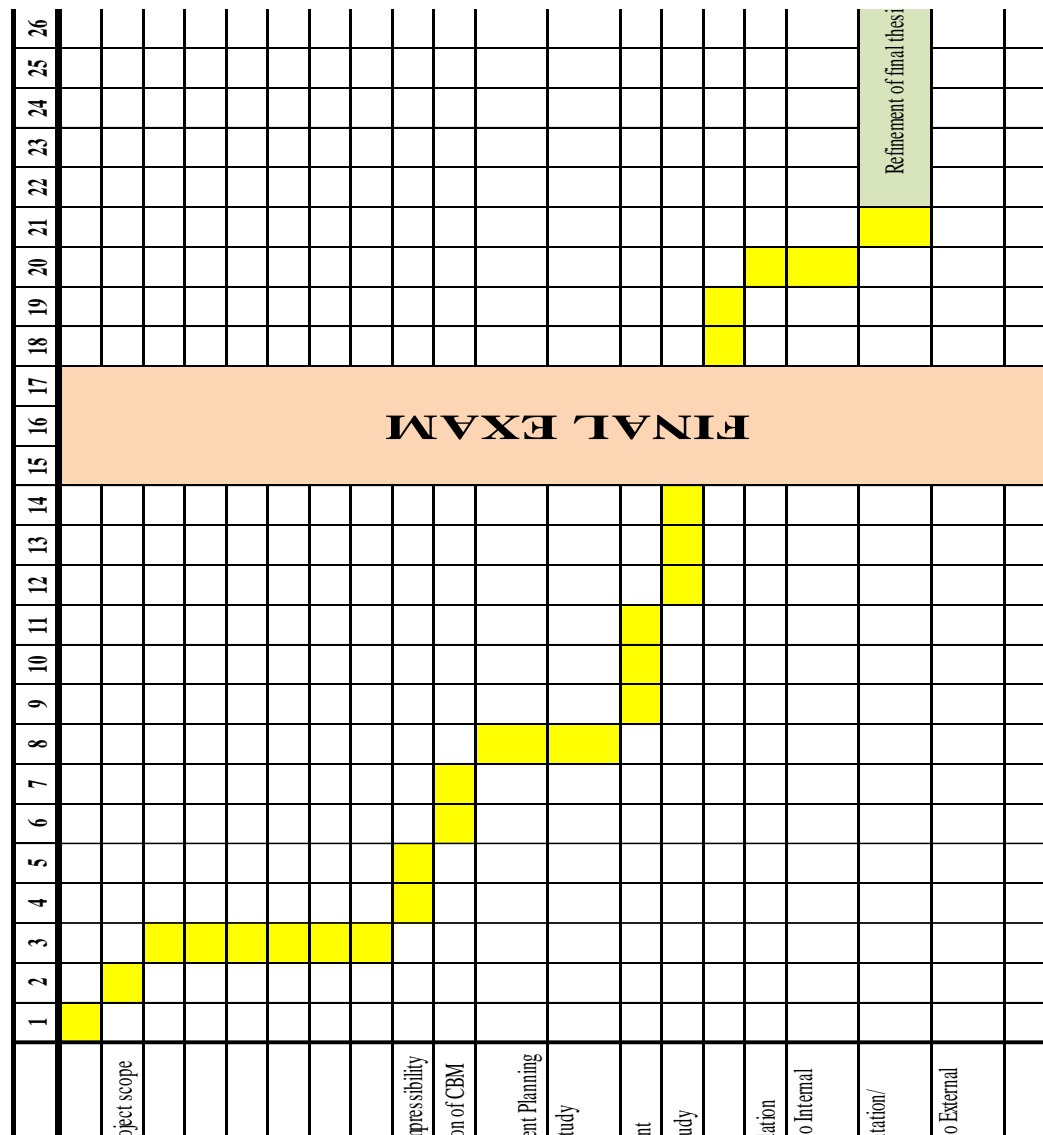


Figure 21 Final Year Project Gantt Chart with Key Milestones and Future Activities

## CHAPTER 4

### EXPECTED RESULTS

Based on previous experiments carried out in the study of coal compressibility, the following are the expected results:

- Matrix compressibility has insignificant impact on the production of CBM from coalbed reservoirs.
- Matrix shrinkage compressibility will result in an increase in production of CBM from coalbed reservoirs.

- Pore compressibility and bulk compressibility will result in a decrease in production of CBM from coalbed reservoirs.
- The increase in production due to matrix shrinkage compressibility has the potential to offset the reduction in production caused by pore compressibility and bulk compressibility.

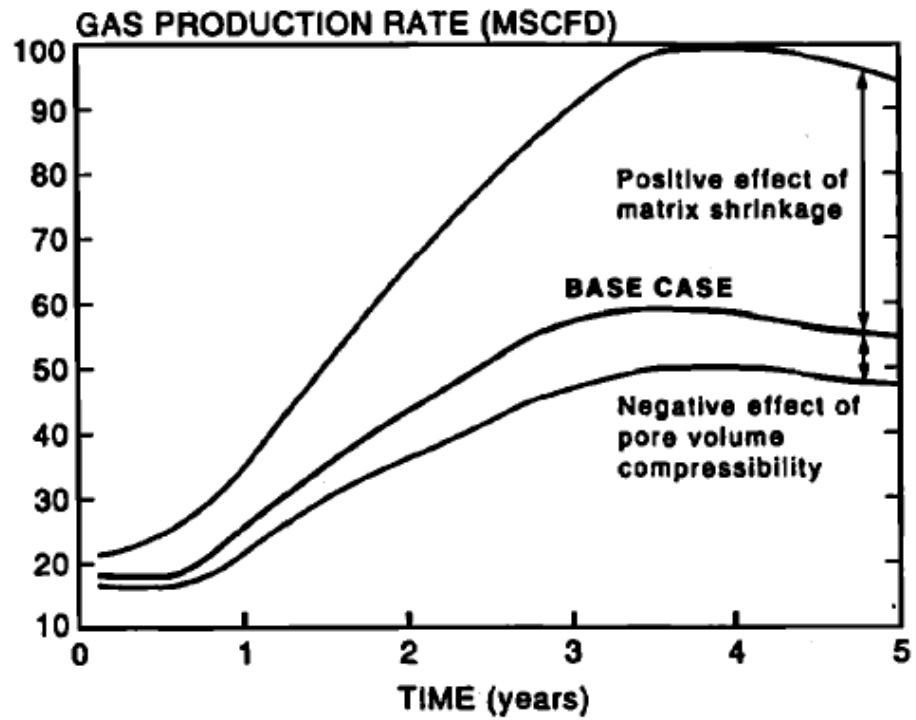


Figure 22 Expected results of effects of compressibilities on gas production rate (Harpalani S. , 1999)

## CHAPTER 5

### RESULTS AND DISCUSSION

#### 5.1 Permeability Test Using PoroPerm

Permeability of a coal field plays an important role in determining if a commercially viable flow rate can be achieved in order for the field to be developed into CBM producing field. While the commercially viable permeability value differs from one field to another, Table 1 shows the generalized classification of permeability values and the corresponding coal field quality:

Permeability Value	Coal Field Production Quality
Less than 0.1	Limited improvement in gas production from fracturing
Between 0.1mD and 1.0mD	Marginal improvement in gas production from fracturing
Between 1.0mD and 10.0mD	Enhanced improvement in gas production from fracturing
10.0mD and above	High gas production with natural fracture

**Table 1 Classification of permeability values with respect to coal field production quality (Rogers, Ramurthy, Rodvelt, & Mullen, 2007)**

Two samples of coal with size of 1.5in x 3in from Sarawak coal field are examined using the PoroPerm device in order to determine the permeability. Three different gases, nitrogen, helium and carbon dioxide are flown through the device separately in order to determine the gas permeability.

Type of Gases	Permeability, mD	
	Sample 1	Sample 2
Carbon Dioxide, CO <sub>2</sub>	7.84	11.03
Nitrogen, N <sub>2</sub>	8.63	9.21
Helium, He	8.04	9.87

**Table 2 Permeability result of Sarawak coal samples**

Permeability result from the test shows that there is a difference of 40.7% between the lowest permeability value (7.84mD) and the highest permeability

value (11.03mD). Also, the result shows that permeability value in Sample 2 is higher than that in Sample 1 for all tests with different gases. The permeability anisotropy can be attributed to the cleating system of the coal samples, given that the network of cleats in these samples should be highly developed as it is a sub-bituminous coal rank(Gash et al, 1992).

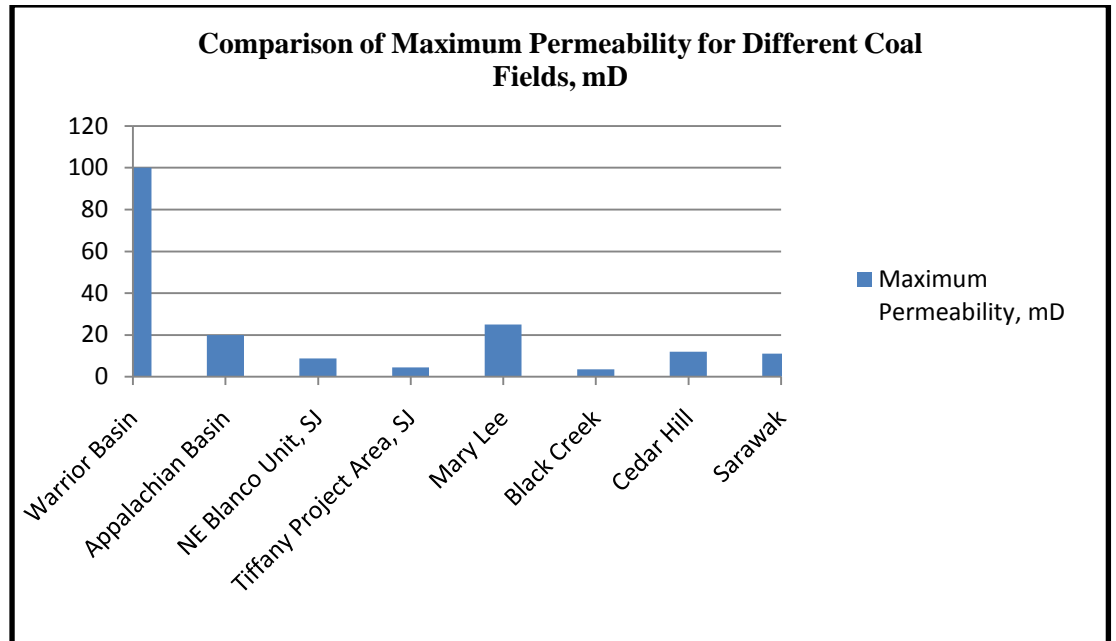


**Figure 23 Comparison of maximum permeability for different coal fields(Rogers, Ramurthy, Rodvelt, & Mullen, 2007)**

Figure 23 illustrates that Sarawak coal field has permeability value higher than some existing producing coal field. However, it also means that the commercial viability of different producing coal fields depends on a large range of permeability.

However, it should be noted that the permeability result this test may not accurately represent the actual coal reservoir permeability. The inaccuracy may be due to the following:

1. Changes in stress will affect the actual reservoir permeability, as discussed in Chapter 3
2. Core samples of coal are not able to sample the complete network of fractures and joints due to its small size. The fractures and joints in the core samples may differ from other region of the coal reservoir.

3. Damages to core during extraction and transportation from the reservoir to the lab may impair the results of the permeability value. For example, due to the fragile nature of coal, the samples may have suffered from induced fracture due to improper handling, resulting in higher permeability results.

## 5.2 Simulation of Various Field Data Using Laboratory Permeability Results

Given the permeability value, several field data that explains the potential of Sarawak coal field as coalbed methane reservoir have been simulated. The simulation uses the input from Table 3:

<b>Input Data</b>	<b>Unit</b>	<b>Value</b>
Pay Zone	ft	30.0
Porosity	%	3.3
Permeability	mD	9.0
Reservoir Depth (Tops)	ft	656
Connate Gas Saturation	%	10
Rock Compressibility	psia <sup>-1</sup>	0.00000138
Water Compressibility	psia <sup>-1</sup>	0.0000209
Gas Density	lb/ft <sup>3</sup>	0.044
Water Density	lb/ft <sup>3</sup>	64.0
Initial Reservoir Pressure	psia	2000
Flowing Bottomhole Pressure	psia	100
Drainage Area	ft <sup>2</sup>	25090.6
Water Viscosity	cp	0.5
Net-to-Gross	-	1.0

**Table 3 Input data for predicting Sarawak coal field CBM production**

Based on the input in Table 3, a 10-year CBM production simulation has been run in order to determine the Gas Production Rate, Water Production Rate, Total Gas Production, Total Water Production and Gas Initial In Place.

## 5.2.1 Gas Production Rate Curve and Water Production Rate Curve

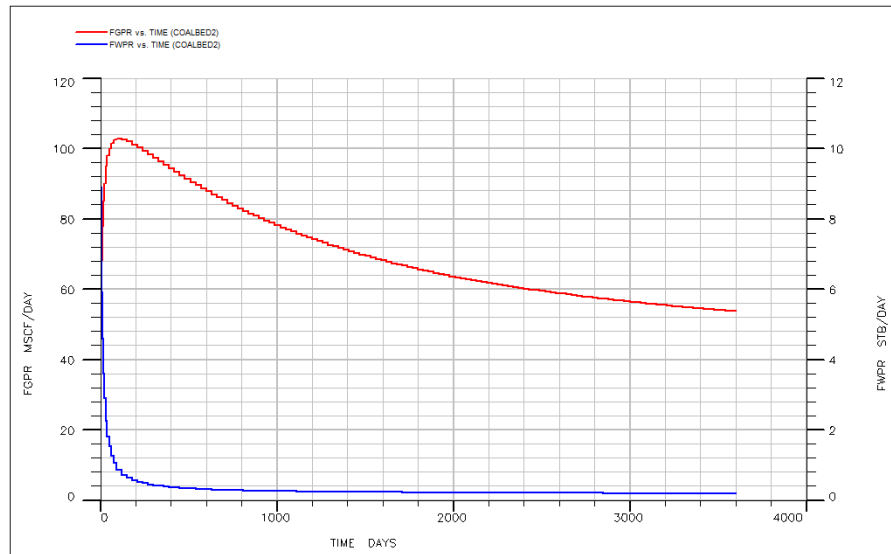


**Figure 24 Simulated gas and water production rate curve of Sarawak coal field**

Figure 24 shows CBM production in Sarawak coal field undergoes three distinct stages. During Stage One, which is probably only the first 25 days of production, CBM well will experience constant water production with limited increase in gas production and limited decline in flowing bottomhole pressure. At this stage, the water aquifer is still strong and the wellbore radius is experiencing steady-state flow.

In Stage Two, which begins at Day 25, water production rate decreases significantly and gas production rate increases exponentially. It is at this stage where the relative permeability of water decreases and the relative permeability of gas increases. ‘Dewatering’ causes the hydrostatic pressure acting on the coal matrices to decrease and gas is desorbed from the coal matrices. Gas production rate increases until it reaches a maximum point called Peak Gas Rate, which is approximately 103 Mscf/day.

Stage Three begins after Peak Gas Rate has been achieved. In this stage, the gas production rate stabilizes and experiences typical decline trend. The low level of water production rate can be explained by the fact that the coal reservoir should be ‘dewatered’ by this stage. Relative permeabilities of both gas and water have achieved plateau



stage and undergo negligible changes. The reservoir is experiencing pseudo-steady state for the remainder of the production lifetime.

### 5.2.2 Total Gas Production Curve and Total Water Production Curve

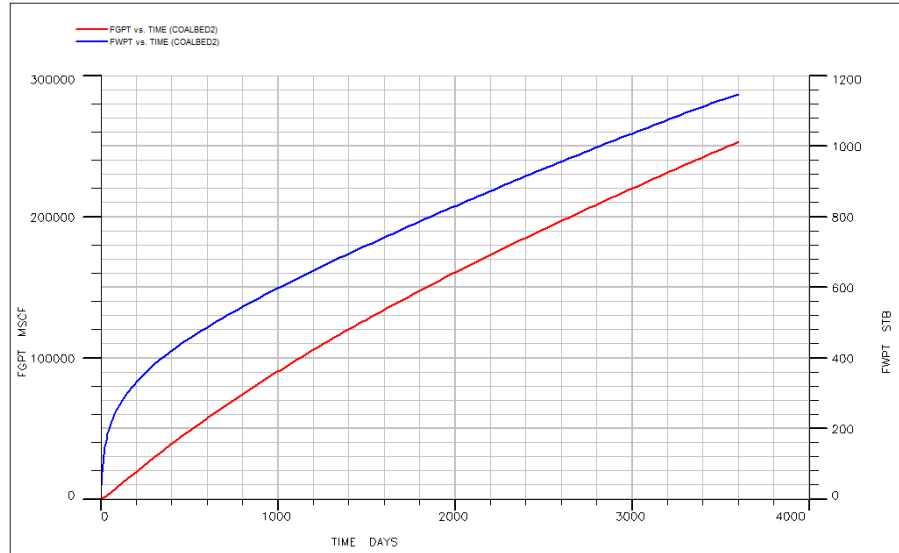


**Figure 25 Simulated cumulative water and gas production curve of Sarawak coal field**

Figure 25 shows the cumulative gas and water production for the first 10 years of the Sarawak coal field. Based on the graph, approximately 250 MMscf of gas can be extracted from the field after 10 years, which is only 20% of the estimated Gas Initial In-Place (GIIP) of the field, as explained in Figure 26.

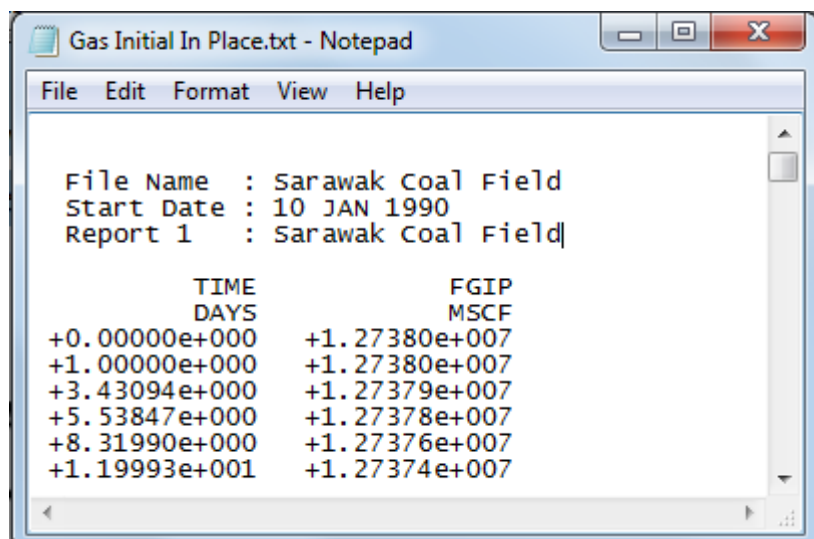


**Figure 26 Simulated GIIP of Sarawak coalfield**

Figure 26 shows the simulated GIIP of the Sarawak coal field. The GIIP is shown on the first row under FGIP (Field Gas In Place) column, i.e.  $1.238 \times 10^7$  Mscf, or equivalent to 12.38 Bscf in an area of  $25090.6 \text{ft}^2$ . This estimated figure is approximately 18.6% different from the estimation by (Kong et al, 2011).

### **5.3 Comparison of Simulation Results to Powder River Basin**

Based on the data obtained from Mavor et al (2003), gas production rate in Powder River Basin is simulated using Eclipse software. The reason Powder River Basin was chosen because it shared a common coal rank as the Sarawak Coal Field, that is sub-bituminous rank. Table 4 shows the data being input into Eclipse to simulate its gas production rate.

Property	Units	Triton Fed. #21C-2623	Twenty Mile #21C-3523
<b>Geometry</b>			
Reservoir Top Depth	feet	557	530
Reservoir Bottom Depth	feet	621	594
Gross Thickness	feet	64	64
<b>Thermal Maturity, Organic and Mineral Composition</b>			
ASTM Coal Rank Classification	-	Subbit. C	Subbit. C
Caloric Value (moist, mineral-matter-free)	Btu/lbm	9,118	9,260
Mean-Maximum Vitrinite Reflectance (in oil)	%	0.42	0.34
Vitrinite Content (mineral-matter-free)	vol. %	73.3	77.7
Inertinite Content (mineral-matter-free)	vol. %	22.5	18.5
Liptinite Content (mineral-matter-free)	vol. %	4.2	3.8
Clay Content (organic-free)	vol. %	83.7	88.2
Carbonate Content (organic-free)	vol. %	trace	trace
Sulfide Content (organic-free)	vol. %	trace	trace
Quartz Content (organic-free)	vol. %	16.3	5.9
<b>Coal Properties</b>			
Moisture Holding Capacity (65 °F)	wt. %	27.49	27.93
Ash Content (moist)	wt. %	4.40	3.83
Sulfur Content (moist)	wt. %	0.16	0.20
Total Density (moist)	g/cm <sup>3</sup>	1.335	1.313
<b>Gas Content, Composition, Sorption Time</b>			
In-Situ Sorbed Gas Content (moist with ash)	scf/ton	22.0	21.7
Sorbed Methane Concentration	mole %	91.16	89.47
Sorbed Ethane Plus Concentration	mole %	0.03	0.02
Sorbed Carbon Dioxide Concentration	mole %	7.39	8.18
Sorbed Nitrogen Concentration	mole %	1.42	2.31
Sorbed Hydrogen Concentration	mole %	0.0	0.02
Sorption Time	hours	42.6	50.7
<b>Gas Storage Capacity</b>			
CH <sub>4</sub> Langmuir Storage Capacity (dry, ash-free)	psia	116.8	107.3
CH <sub>4</sub> Langmuir Storage Capacity (in-situ)	psia	79.37	73.0
CH <sub>4</sub> Langmuir Pressure	scf/ton	394	358
CO <sub>2</sub> Langmuir Storage Capacity (dry, ash-free)	scf/ton	1,722.4	1,306.9
CO <sub>2</sub> Langmuir Storage Capacity (in-situ)	scf/ton	1,171.8	889.2
CO <sub>2</sub> Langmuir Pressure	psia	791	481
In-Situ Mixture Storage Capacity	scf/ton	23.7	23.0
<b>Reservoir Temperature and Pressure</b>			
Average Temperature	°F.	65	65
Pressure Gradient to Surface	psi/ft	0.237	0.240
Initial Pressure	psia	152.5	147.6
Pressure Depth	feet	589	562
Critical Desorption Pressure	psia	137.8	115.3
<b>Natural Fracture System</b>			
Absolute Permeability	md	632 to 3,160	nm

Table 4 Coal Properties of Powder River Basin (Mavor et al, 2003)

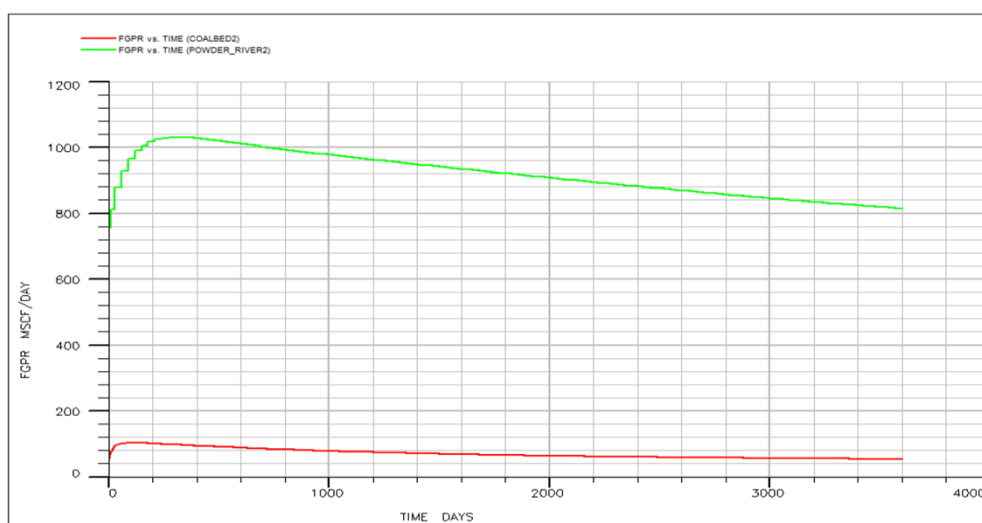


Figure 27 Comparison of Gas Production Rate of Sarawak Coal Field and Powder River Basin

Figure 27 shows CBM production in Sarawak coal field and Powder River Basin. For Powder River Basin, its stage one also lasted approximately for a month's time in which the wellbore radius is experiencing steady state flow. In Stage Two, Powder River Basin achieves its Peak Gas Rate at approximately 1038Mscf/day. However, this Peak Gas Rate is only achieved sometime around 300 days after production has begun. Thereafter, it underwent Stage Three where the gas production rate stabilizes and experiences typical decline.

From the comparison, both Powder River Basin and Sarawak Coal Field exhibit similar trend in its gas production rate pattern. However, the higher value of the Powder River Basin is due to the larger surface area and thickness of its coalbed as compared to Sarawak Coal Field. The production capacity of Powder River Basin is approximately 10 times larger than the production potential of Sarawak Coal Field.

#### 5.4 Relationship between Stress Changes and Permeability

A stress test was conducted using Single Point Load Test in order to determine the strength of the rock. In this test, a load is exerted on the coal samples until the coal samples have been crushed. A total of five samples were used and the results are shown in Table 5:

<b>Samples</b>	<b>1</b>	<b>2</b>	<b>3</b>	<b>4</b>	<b>5</b>
Crush Load (psi)	562	463	511	487	542
Crush Load (MPa)	3.87	3.19	3.52	3.35	3.74

**Table 5 Single Point Load Testing Results**

By using the following formula, permeability of coal versus load is interpolated (Gray, 1987):

$$k = 1.013 \times 10^{-031n}$$

**Equation 16**

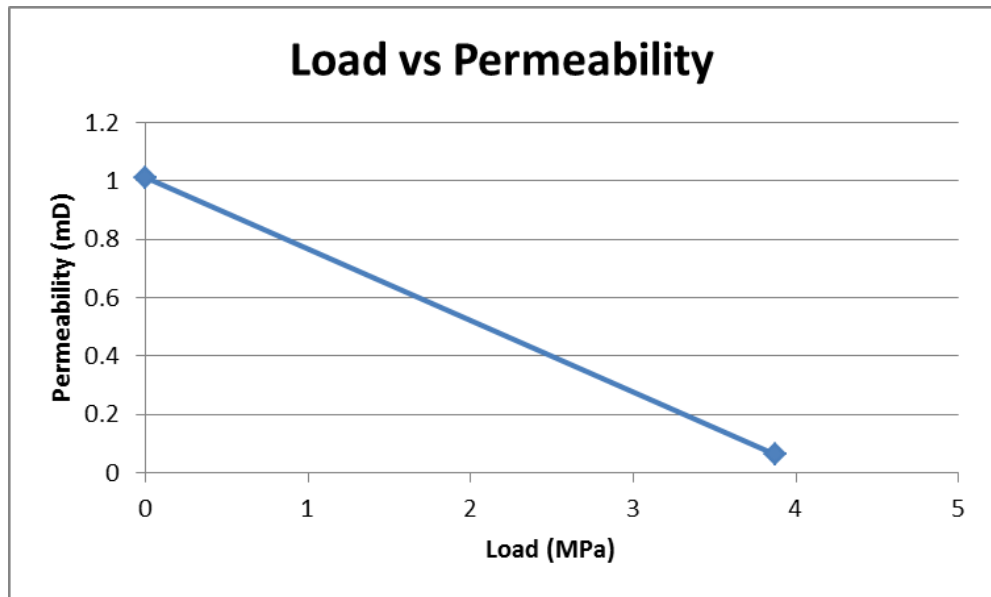


**Figure 28 Load vs Permeability**

Figure 28 illustrated how during production, ‘dewatering’ increases the net effective stresses acting on the coal structure, hence, fissures and pore spaces in the coal structure tend to be compressed. As gas tends to flow through the pore spaces, a compaction of these spaces due to higher net effective stress will result in lower channel for gas to flow through, ultimately resulting in lower flowrate. Net effective stress refers to the difference in overburden pressure and hydrostatic pore pressure from the coal. Carmen-Kozeny correlation also argues that since rock matrix such as coal is incompressible, all volume changes due to compression only affects the pore spaces (McKee et al, 1987). Experiments conducted using black coal displayed that the permeability of coal is highly affected by stress. Permeability reduces steeply with an increase in effective stress acting on it, and vice versa (Somerton et al, 1975 and McKee et al, 1987).

## CHAPTER 6

### CONCLUSION AND RECOMMENDATIONS

#### 6.1 Conclusion

Based on the simulation of Sarawak coalfield, it can be concluded that it has a prospective potential to be developed as a CBM field. This is based on the GIIP value of 12.38 Bscf obtained via simulation and a laboratory permeability value of 8.0mD – 11.5mD, which corresponds with increased production after fracturing.

Also, permeability decreases with an increase in net effective stress. This is due to the compaction of pore spaces that form the channel for gas to flow through during production.

Matrix adsorption effect on permeability cannot be conducted in this project due to the limitation of equipment within the university.

#### 6.2 Recommendations

Future recommendations are proposed in order to improve the accuracy of this experiment:

- Permeability of coal samples should be obtained using triaxial cell fitted with gas permeability measurement.
- Coring of 15cm x 11cm samples should be done using aero-coring machine. However, UTP only has hydro-coring machine, which was not able to core the sample size as coals are easily broken due to its fragile nature.

## Nomenclature

$Q$	=	Quantity of gas in fracture, scf
$\Phi$	=	Coal porosity, %
$A$	=	Area, ft <sup>2</sup>
$h$	=	Net pay, ft
$S_w$	=	Water saturation, %
$B_g$	=	Formation volume factor of gas, ft <sup>3</sup> /scf
$Q$	=	Quantity of gas adsorbed at a given pressure $p$ , scf/ton
$V_L$	=	Langmuir volume parameter, scf/ton
$P_L$	=	Langmuir pressure parameter, psia
$P$	=	Pressure, psia
$M$	=	Mass flowrate, gm <sup>-1</sup> s <sup>-1</sup>
$D$	=	Diffusion coefficient, m <sup>2</sup> s <sup>-1</sup>
$\Delta C$	=	Concentration gradient, gm <sup>-3</sup>
$M$	=	Mass flowrate, gm <sup>-1</sup> s <sup>-1</sup>
$\rho$	=	Gas density, g/m <sup>3</sup>
$k$	=	Apparent permeability of coal, m <sup>2</sup>
$\mu$	=	Viscosity of gas, cp
$\nabla P$	=	Pressure gradient, Pa
$C_b$	=	Bulk compressibility, psi <sup>-1</sup>
$V_b$	=	Bulk volume, in <sup>3</sup>
$dV_b$	=	Change in bulk volume, in <sup>3</sup>
$dP_e$	=	Change in external pressure, psi
$C_{ms}$	=	Matrix shrinkage compressibility, psi <sup>-1</sup>
$V_m$	=	Matrix volume, in <sup>3</sup>
$dV_m$	=	Change in matrix volume, in <sup>3</sup>
$dP_s$	=	Change in pressure of sorbing gas, psi
$C_m$	=	Matrix compressibility, psi <sup>-1</sup>
$V_m$	=	Matrix volume, in <sup>3</sup>

$dV_m$	=	Change in matrix volume, in <sup>3</sup>
$dP$	=	Change in external pressure and internal pressure, psi
$C_p$	=	Pore compressibility, psi <sup>-1</sup>
$V_p$	=	Pore volume, in <sup>3</sup>
$dV_p$	=	Change in pore volume, in <sup>3</sup>
$dP_i$	=	Change in internal pressure, psi
$n$	=	Load, MPa



## Bibliography

1. Alberta Energy. (2013). *About Coalbed Methane*. Retrieved 13 February, 2013, from Alberta Energy: <http://www.energy.alberta.ca/naturalgas/754.asp>
2. Aminian, K. (2007). *Coalbed Methane - Fundamental Concepts*. Petroleum & Natural Gas Engineering Department, West Virginia University.
3. Anderson, J. e. (2003). Producing Natural Gas From Coal. *Oilfield Review*, pp. 9-31.
4. Australia Science Media Center. (2012). *Coal Seam Gas In A Nutshell*. New South Wales: Science In A Nutshell.
5. Australian Coal Association Research Program. (2013). *Rank of Coal Seam*. Retrieved 14 February, 2013, from [www.undergroundcoal.com.au](http://www.undergroundcoal.com.au): <http://www.undergroundcoal.com.au/outburst/rank.aspx>
6. Dunn, B. (1989). Coal As A Conventional Source of Methane: A Review and Analysis of 50 Wells in Two Production Areas in the Black Warrior Basin of Alabama. *SPE/DOE/GRI Unconventional Gas Recovery Symposium*. Pittsburgh: Society of Petroleum Engineers of AIME.
7. Fekete Associates Inc. (2011). *CBM Concepts*. Retrieved from Fekete - Reservoir Engineering Software and Services: <http://www.fekete.com/software/cbm/media/webhelp/c-te-concepts.htm>
8. Gash, B. (1992). The Effects of Cleat Orientation and Confining Pressure on Cleat Porosity, Permeability and Relative Permeability in Coal. *SCA Conference*.
9. Gray, I. (1987). Reservoir Engineering in Coal Seams: Part I: The Physical Process of Gas Storage and Movement in Coal Seams. *SPE Reservoir Engineering*.
10. Gregg, S. (1961). *The Surface Chemistry of Solids*. New York: Reinhold Publishing Corp.
11. Gu, F., & Chalaturnyk, R. (2006). Numerical Simulation of Stress and Strain Due to Gas Sorption/Desorption and Their Effects on In Situ Permeability of Coalbeds. *Journal of Canadian Petroleum Technology*, 52-62.
12. Harpalani, S. (1999). Compressibility of Coal and Its Impact On Gas Production from Coalbed Reservoirs. In Amadei, Kranz, Scott, & Smeallie, *Rock Mechanics for Industry* (pp. 301-308). Rotterdam: Balkema.
13. Harpalani, S., & Schraufnagel, R. (1990). Influence of Matrix Shrinkage and Compressibility on Gas Production from Coalbed Methane Reservoirs. *65th*

*Annual Technical Conference and Exhibition*. New Orleans: Society of Petroleum Engineers.

14. Harpalani, S., Zhao, X., & Farmer, I. (1991). *The Mechanics of Gas Flow in Coal - A Laboratory Investigation*. International Society for Rock Mechanics.
15. Irawan, S., Nair, P., & Tunio, S. Q. (2012). Forecasting CBM Production of Mukah Balingian Coalfield, Sarawak, Malaysia. *Research Journal of Applied Sciences, Engineering and Technology*, 4265-4274.
16. Jasinge, D., Ranjith, P., & Choi, S. (2010). Effects of Effective Stress Changes on Permeability of Latrobe Valley Brown Coal. *Fuel* 90, 1292-1300.
17. Kong, C. (2011). Preliminary Study on Gas Storage Capacity and Gas-in-Place for CBM Potential in Balingian Coalfield, Sarawak Malaysia. *International Journal of Applied Science and Technology*, 82-94.
18. Langmuir, I. (1918). The Adsorption of Gases on Plane Surfaces of Glass, Mica and Platinum. *American Chemical Society*, 40, 1361-1403.
19. Laubach, S., & Tremain, C. (1991). Regional Coal Fracture Patterns and Coalbed Methane Development. In J. Roegiers, *32nd Symposium on Rock Mechanics* (pp. 851-859). Rotterdam: Balkema.
20. Laubach, S., Marrett, R., Olson, J., & Scott, A. (1997). Characteristics and Origins of Coal Cleat: A Review. *International Journal of Coal Geology*, 175-207.
21. Moffat, D., & Weale, K. (1955). Sorption by Coal of Methane At High Pressure. *Fuel*, pp. 449-462.
22. McKee, C. B., Bumb, A.C., Koenig, R. A. (1987). Stress Dependent Permeability and Porosity of Coal and Other Geologic Formation. *International Coalbed Methane Symposium*, (pp. 183-193). Alabama.
23. Mavor, M.J., Russell, B., Pratt, T.J. (2003). Powder River Basin Ft. Union Coal Reservoir Properties and Production Decline Analysis, *SPE Annual Technical Conference and Exhibition*, Denver
24. Puri, R., Evanoff, J., & Brugler, M. (1991). Measurement of Coal Cleat Porosity and Relative Permeability Characteristics. *SPE Gas Technology Symposium* (pp. 93-104). Society of Petroleum Engineers.
25. Rabia, H. (1988). *Mine Environmental Engineering*. Newcastle: Entrac Software.

26. Rogers, R., Ramurthy, M., Rodvelt, G., & Mullen, M. (2007). *Coalbed Methane Principles & Practices* (Third ed.). Starkville, MS: Oktibbeha Publishing Co.
27. S, R., Gonzalez, R., A.M.G., K., Fitzgerald, J., Pan, Z., Sudibandriyo, M., et al. (2005). Measurement and Prediction of Single- and Multi-Component Methane, Carbon Dioxide and Nitrogen Isotherms for U.S. Coals. *International Coalbed Methane Symposium*.
28. Schlumberger System Information Support (2008). The Coal Bed Methane Model. In Schlumberger, *Eclipse Technical Description* (pp. 124-156).
29. Seidle, J., Jeansonne, M., & Erickson, D. (1995). Application of Matchstick Geometry to Stress Dependent Permeability in Coals. *International Meeting on Petroleum Engineering*. Beijing: Society of Petroleum Engineers.
30. Somerton, W. S. (1975). Effect of Stress on Permeability of Coal. *Int J Rock Mech Min Sci Geomech*, 129-145.
31. Stopa, J., & Nawrat, S. (2012). Computer Modeling of Coalbed Methane Recovery in Coal Mines. *Journal of Energy Resources Technology*.
32. Strickland, T., Logan, S. D., & Wickstrom, L. (2008). *Coal*. Ohio: Ohio Geological Survey.
33. Van Golf-Racht, T. (1982). *Fundamentals of Fractured Reservoir Engineering*. New York: Elsevier Scientific Publishing Co. Inc.
34. Warren, J., & Root, P. (1963). The Behaviour Of Naturally Fractured Reservoir. In *Society of Petroleum Engineers Journal* (pp. 245-255). Gulf Research and Development Co.
35. Wei, X., Wang, G., Massaroto, P., & Golding, S. (2006). A Case Study on the Numerical Simulation of Enhanced Coalbed Methane Recovery. *SPE Asia Pacific Oil and Gas Conference and Exhibition 2006*. Adelaide: Society of Petroleum Engineers.
36. Zeng, K., Xua, J., Heb, P., & Wang, C. (2011). Experimental Study on Permeability of Coal Sample Subjected to Triaxial Stress. *First International Symposium on Mine Safety Science and Engineering* (pp. 1051-1057). Elsevier Ltd.